JMEPEG (2009) 18:182–189
DOI: 10.1007/s11665-008-9276-7

1059-9495/$19.00

Interfacial Reactions and Bonding Strength of Sn-*x*Ag-0.5Cu/Ni BGA Solder Joints

K.S. Lin, H.Y. Huang, and C.P. Chou

(Submitted September 7, 2007; in revised form June 2, 2008)

The present study details the microstructure evolution of the interfacial intermetallic compounds (IMCs) layer formed between the Sn-*x*Ag-0.5Cu (*x* = 1, 3, and 4 wt.%) solder balls and electroless Ni-P layer, and their bond strength variation during aging. The interfacial IMCs layer in the as-reflowed specimens was only $(Cu,Ni)_6Sn_5$ for Sn-*x*Ag-0.5Cu solders. The $(Ni,Cu)_3Sn_4$ IMCs layer formed when Sn-4Ag-0.5Cu and Sn-3Ag-0.5Cu solders were used as aging time increased. However, only $(Cu,Ni)_6Sn_5$ IMCs formed in Sn-1Ag-0.5Cu solders, when the aging time was extended beyond 1500 h. Two factors are expected to influence bond strength and fracture modes. One of the factors is that the interfacial $(Ni,Cu)_3Sn_4$ IMCs formed at the interface and the fact that fracture occurs along the interface. The other factor is Ag_3Sn IMCs coarsening in the solder matrix, and fracture reveals the ductility of the solder balls. The above analysis indicates that during aging, the formation of interfacial $(Ni,Cu)_3Sn_4$ IMCs layers strongly influences the pull strength and the fracture behavior of a solder joint. This fact demonstrates that interfacial layers are key to understanding the changes in bonding strength. Additionally, comparison of the bond strength with various Sn-Ag-Cu lead-free solders for various Ag contents show that the Sn-1Ag-0.5Cu solder joint is not sensitive to extended aging time.

Keywords ball pull test, bonding strength, interface, lead-free solder, Sn-Ag-Cu

1. Introduction

In response to increasing concerns about the environmental impact of lead-bearing products, many studies on the development and improvement of lead-free solder alloys have been performed since the early 1990s. Among various lead-free candidate alloys, the Sn-Ag-Cu alloy family is preferred for combination with other alloys (Ref 1-3), offering advantages of favorable wetting properties, high mechanical strength, and high creep resistance (Ref 4).

The soldering process and normal wear can cause various interfacial reactions between solders and metallic substrates, forming intermetallic compounds (IMCs). A thin, continuous and uniform IMC layer can cause wetting and improve the joint strength, to secure joint-ability during the service life of products (Ref 5). However, the formation of excessive IMCs at the interface can degrade the overall performance of a solder joint because of the brittleness of IMCs and their thermal mismatch with neighboring materials (Ref 6, 7).

Many studies have been performed on the interfacial reaction between Sn-Ag-Cu or Sn-Cu lead-free solders and the Ni layer or the Ni-P layer during reflow or aging (Ref 1-3, 6-10). In the interfacial reaction, $(Cu,Ni)_6Sn_5$ and/or $(Ni,Cu)_3Sn_4$ IMCs, which comprise Cu, Ni, and Sn, were observed. He et al. (Ref 11, 12) described the solid-state interfacial reaction of Sn-based solders with the Ni-P layer. They found three distinctive layers, Ni_3Sn_4, NiSnP, and Ni_3P, between Sn-containing solders and the Ni-P layer. Yoon et al. (Ref 9) and others (Ref 6) found that the consumption of Ni by the formation of the $(Ni,Cu)_3Sn_4$ IMC layer was such that P was expelled to the remaining Ni-P layer and formed the Ni_3P layer. Related references reveal that results concerning IMC phases and IMC compositions from reactions among Ni, Cu, and Sn at the interface are very complicated. The weakening of the Ni_3Sn_4/solder interface with aging is a complex phenomenon and has always been a focus of interest. Several investigations have already identified the brittleness of Ni_3Sn_4 and the formation of Kirkendall voids has been cited as a reason for the decrease in shear strength (Ref 4, 8). In another study, the excess growth of a P-rich layer was found to degrade the joint strength because of the presence of brittle Ni_3P compounds in the layer (Ref 10, 13). However, relatively little research has been performed on pull strength degradation with aging time.

This work compares the solid-state interfacial reactions of Ni-P with various Sn-Ag-Cu lead-free solders for various Ag contents, to establish a comprehensive database of solid-state reactions of Ni-P with Sn-*x*Ag-0.5Cu solders. Also, pull strength tests were performed to evaluate the effect of the interfacial reactions on the reliability of the solder joints as a function of aging time.

2. Experimental

Three types of solder balls investigated in this study were the Sn-1.0Ag-0.5Cu, Sn-3.0Ag-0.5Cu, and Sn-4.0Ag-0.5Cu

K.S. Lin and **C.P. Chou**, Department of Mechanical Engineering, National Chiao Tung University, Hsinchu 300, Taiwan; and **H.Y. Huang**, Department of Materials Science and Engineering, National Formosa University, Yunlin 632, Taiwan. Contact e-mail: huanghy@nfu.edu.tw.

solders with diameter of 0.45 mm. The substrate used was a copper pad deposited with electroless Ni-P immersion Au surface finish. The thicknesses of Au and Ni layers were 0.05 and 2.54 μm, respectively. The solder balls were dipped in rosin mildly activated (RMA) flux, placed on the Au/Ni-P/Cu pads, and then reflowed in an IR reflow oven with nine different zones. The reflow temperature profile with the peak temperature was set at 240 °C, and the soaking time above 190 °C was about 90 s. After solder reflow, samples reflowed were cooled at 5 °C s^{-1} to room temperature in the reflow oven. Certain reflowed ball grid array (BGA) packages were further aged at 150 °C for various times ranging from 100 to 1500 h.

The reflowed and aged specimens were cross sectioned through a row of solder balls, ground with SiC paper, and polished with 0.1 μm diamond paste. The microstructure was observed via scanning electron microscopy (SEM), and chemical compositions were analyzed using an energy-dispersive X-ray spectrometer (EDX) installed in the SEM. An operating voltage of 20 keV was used to characterize the microstructures and phases formed in these solder joints.

The bond strengths of the solder balls on the Au/Ni-P/Cu pads under reflow and various aging conditions were evaluated via ball pull tests which conform to JEDEC Standard JESD22-B115. For this purpose, the ball pull rate was fixed at 0.1 mm/s. An average value was taken from 30 measurements for each condition. After the ball pull tests, the top views of fracture surfaces were investigated thoroughly by SEM as well as EDX.

3. Results and Discussion

Figure 1 presents the SEM micrographs of the interface between Sn-*x*Ag-0.5Cu solders and the Ni-P layer after reflowing. The back-scattered electron image mode of SEM was adopted to provide more distinguishable phase boundaries of the interfacial layers. During reflowing, the topmost Au layer dissolved into the molten solder, leaving the Ni layer exposed to the molten solder. The microstructure of Sn-*x*Ag-0.5Cu solder matrix after reflow contained Ag_3Sn and Cu_6Sn_5 IMCs. Typical scallop-shape IMCs formed at both solder/Ni-P interfaces after reflow. The interfacial IMCs are $(Cu,Ni)_6Sn_5$ phase for Sn-4Ag-0.5Cu solders, as presented in Fig. 1(a). The microstructures of Sn-3Ag-0.5Cu and Sn-1Ag-0.5Cu solder balls after reflow are similar to those of the Sn-4Ag-0.5Cu specimen, and are shown in Fig. 1(b) and (c), respectively. However, the amount of the matrix IMCs decreases as the Ag content is reduced. Additionally, binary $AuSn_4$ IMCs appeared in the solder matrix. These $AuSn_4$ IMCs are produced by the rapid dissolution of the Au film on the Ni-P layer during reflow and the ensuing reaction with the molten solder. After aging at 150 °C, the Sn-*x*Ag-0.5Cu solder joint is seen to contain coarsened Ag_3Sn particles. Some plate-like and gigantic Ag_3Sn IMCs were also observed in the Sn-4Ag-0.5Cu solder matrix after aging for 1500 h, as revealed in Fig. 2(a). Figure 2(b) and (c) reveals that the coarsening of Ag_3Sn precipitates was much slower in the aged Sn-3Ag-0.5Cu and Sn-1Ag-0.5Cu specimens. Furthermore, no plate-like Ag_3Sn IMC is observed in the solder matrix of the Sn-3Ag-0.5Cu and Sn-1Ag-0.5Cu solder joints.

Figure 3 presents the magnified cross-sectional image of the interface between Sn-4Ag-0.5Cu solder and Ni-P layer that had been aged at 150 °C for various periods. After aging for 100 h,

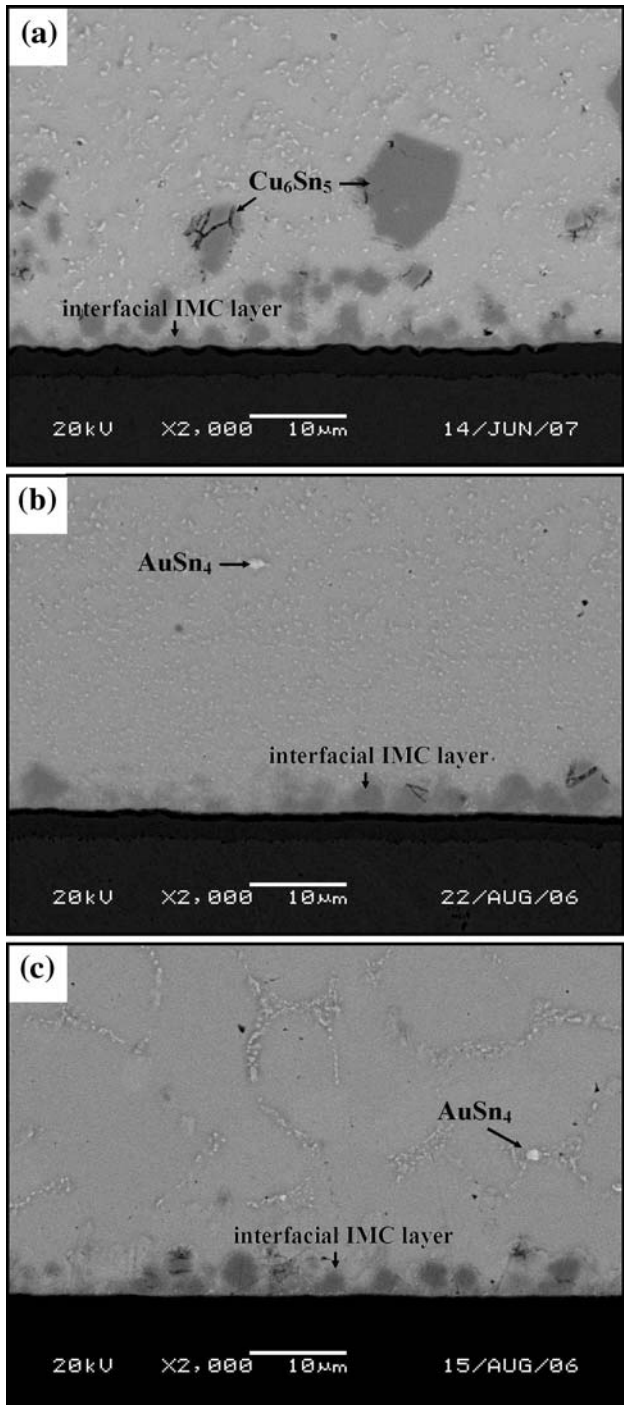

Fig. 1 Microstructure of Sn-*x*Ag-0.5Cu solder balls after reflowing: (a) x = 4.0 wt.%, (b) x = 3.0 wt.%, and (c) x = 1.0 wt.%

an extra IMCs layer appeared between the $(Cu,Ni)_6Sn_5$ IMCs and the Ni-P layer as shown in Fig. 3(a). The EDX analysis identifies the composition of the new IMC layer as Sn-Ni-Cu. The ratio of the atomic percentage of (Ni + Cu) to Sn was close to 3:4. Thus, the reaction layer adjacent to the Ni-P layer could be denoted as $(Ni,Cu)_3Sn_4$ IMC. Jeon et al. (Ref 14) reported the $(Cu,Ni)_6Sn_5$ phase seems to be the most equilibrium phase in the Cu-Ni-Sn ternary system. The $(Ni,Cu)_3Sn_4$ IMC was formed beneath the $(Cu,Ni)_6Sn_5$ IMC because of Cu consumption. They also identified $(Ni,Cu)_3Sn_4$ IMC were the same as

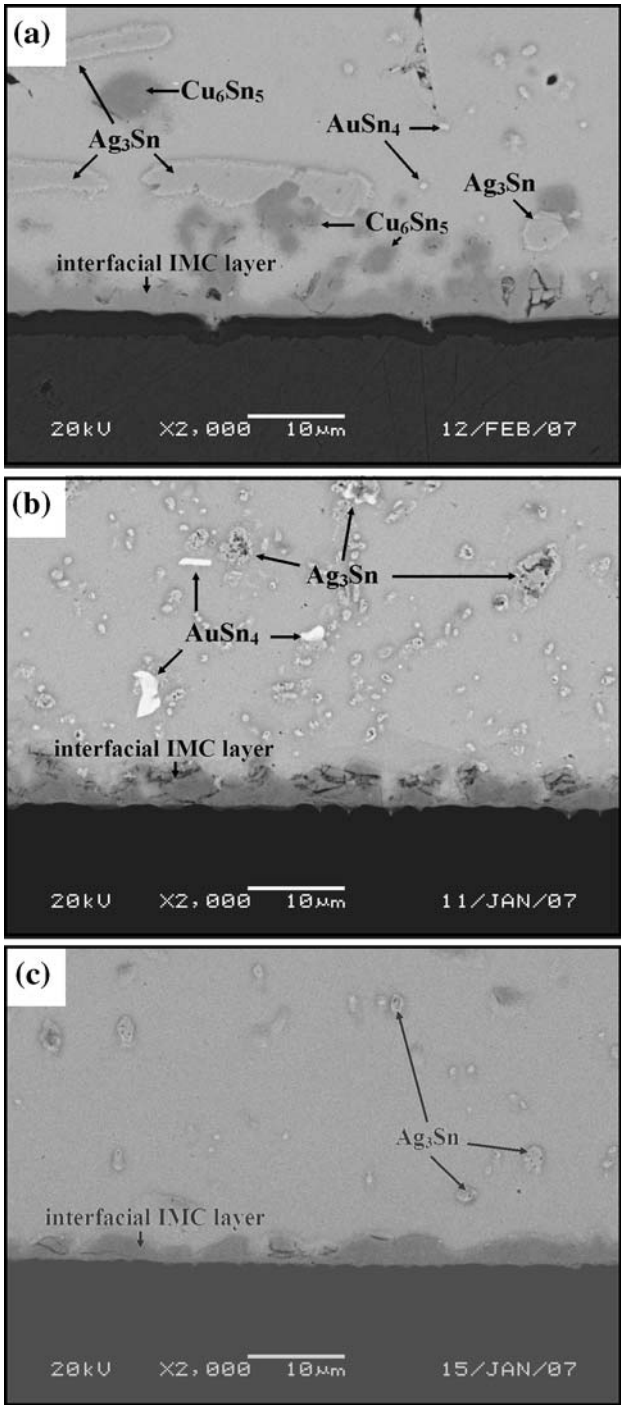

Fig. 2 Microstructure of Sn-*x*Ag-0.5Cu solder balls after aging at 150 °C for 1500 h: (a) x = 4.0 wt.%, (b) x = 3.0 wt.%, and (c) x = 1.0 wt.%

the crystal structure of the Ni_3Sn_4 phase that consists of the Ni_3Sn_4 crystal structure with 4-7 at.% Cu atoms in the Ni sublattice. Figure 3(b) presents the microstructure of the interfacial IMC layers after aging for over 500 h. A single $(Ni,Cu)_3Sn_4$ IMCs layer was present at the interface between the solder and the Ni-P layer. However, the original $(Cu,Ni)_6Sn_5$ IMC was not observed. This result is similar to that of Yoon et al. (Ref 9), who experimentally studied the interfacial microstructures of the ENIG/Sn-3.5Ag-0.7Cu/ENIG sandwich solder joint after aging at 150 °C for over 500 h. When the $(Ni,Cu)_3Sn_4$ IMCs layer appeared in the interface reaction layer, Ni-Sn-P and P-rich layer appeared at the interface between the $(Ni,Cu)_3Sn_4$ IMCs and the Ni-P layer. The P-rich layer formed as Ni was consumed in the formation of the $(Ni,Cu)_3Sn_4$ IMC layer, and P was expelled to the remaining Ni-P layer thus formed in the upper Ni-P layer, and the diffusion reaction process of Sn atoms into P-rich layer results in the Ni-Sn-P layer formation between the P-rich layer and the interfacial $(Ni,Cu)_3Sn_4$ IMC layer (Ref 15). Several reports already revealed that the excess growth of a P-rich layer degrades joint strength because of the presence of brittle Ni_3P compounds in the layer (Ref 10, 13), and in another study (Ref 15), Ni-Sn-P layer had a detrimental effect on the reliability of solder joints. Figure 4 presents the microstructure of the interfacial IMC layers between the Sn-3Ag-0.5Cu solder and the Ni-P layer after aging at 150 °C for various periods. After aging for 100 h, only $(Cu,Ni)_6Sn_5$ IMCs were observed at the interface between the solder and the Ni-P layer, as shown in Fig. 4(a). After prolonged aging for over 500 h, the interface reaction between the solder and the Ni-P layer formed two IMC phases, $(Cu,Ni)_6Sn_5$ and $(Ni,Cu)_3Sn_4$, as presented in Fig. 4(b). The $(Ni,Cu)_3Sn_4$ IMC layer was also observed adjacent to the Ni-P layer, and $(Cu,Ni)_6Sn_5$ IMCs were observed between the $(Ni,Cu)_3Sn_4$ IMCs layer and the solder. After aging for over 1000 h, the $(Ni,Cu)_3Sn_4$ IMCs layer had grown thicker. However, the thickness of the total interfacial reaction layers did not change much with increased aging time. Figure 4(d) presents the microstructure of the Sn-3Ag-0.5Cu sample that had been aged for 1500 h. A comparison with the sample that had been aged for 1000 h reveals that the IMCs that formed at the interfaces changed from $(Cu,Ni)_6Sn_5/(Ni,Cu)_3Sn_4$ double reaction layers to a single $(Ni,Cu)_3Sn_4$ layer. In this case, when $(Ni,Cu)_3Sn_4$ IMCs were observed at the interface reaction layer, an Ni-Sn-P and P-rich layer was formed at the interface between the $(Ni,Cu)_3Sn_4$ IMCs and the Ni-P layer.

Figure 5 presents the microstructure of the Sn-1Ag-0.5Cu/Ni-P interface aged at 150 °C for various periods. After aging for 100-1500 h, the interface reaction formed single $(Cu,Ni)_6Sn_5$ IMCs. This result is consistent with the results for the interfacial reactions of Sn-0.7Cu with Au/Ni/Cu substrate after aging at 70-150 °C (Ref 16). Additionally, with increasing aging time, the thickness of the $(Cu,Ni)_6Sn_5$ IMCs layer increased slightly. In this case, the P-rich layer is detected at the interface between the $(Cu,Ni)_6Sn_5$ IMCs and the Ni-P layer, but no Ni-Sn-P layer is found. This result differs from that in the case of Sn-4Ag-0.5Cu and Sn-3Ag-0.5Cu solder balls. However, Huang et al. (Ref 15) observed similar results for the formation of Ni-Sn-P under the interfacial Ni_3Sn_4 IMC layers, but not under the interfacial $(Cu,Ni)_6Sn_5$ IMC layers.

The reaction products for the different solders and aging times are summarized in Table 1. Two IMC phases, $(Ni,Cu)_3Sn_4$ and $(Cu,Ni)_6Sn_5$, appeared either alone or simultaneously, depending on the solders and the aging times. After reflow, only a layer of $(Cu,Ni)_6Sn_5$ IMCs at the interface of each sample was observed as illustrated in Table 1. A recently established Cu-Ni-Sn ternary isotherm at 235 °C, shown in Fig. 6 (Ref 7), provides rationalization for reaction products. The temperature of the isotherm at 235 °C is quite close to the temperature used in this study for the reflow (at 240 °C), and the isotherm should provide a good approximation. According to this isotherm, the phase fields that are in equilibrium with the molten Sn phase [denoted as (Liquid)] include one three-phase field,

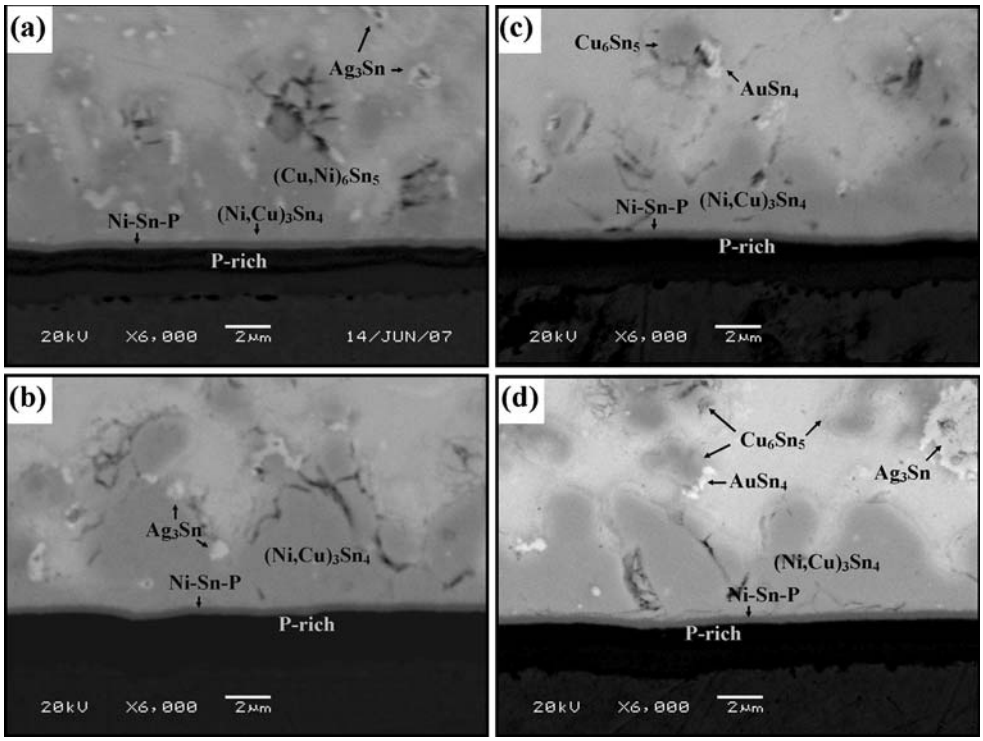

Fig. 3 Microstructure of Sn-4Ag-0.5Cu solder interface after various aging times: (a) 100 h, (b) 500 h, (c) 1000 h, and (d) 1500 h

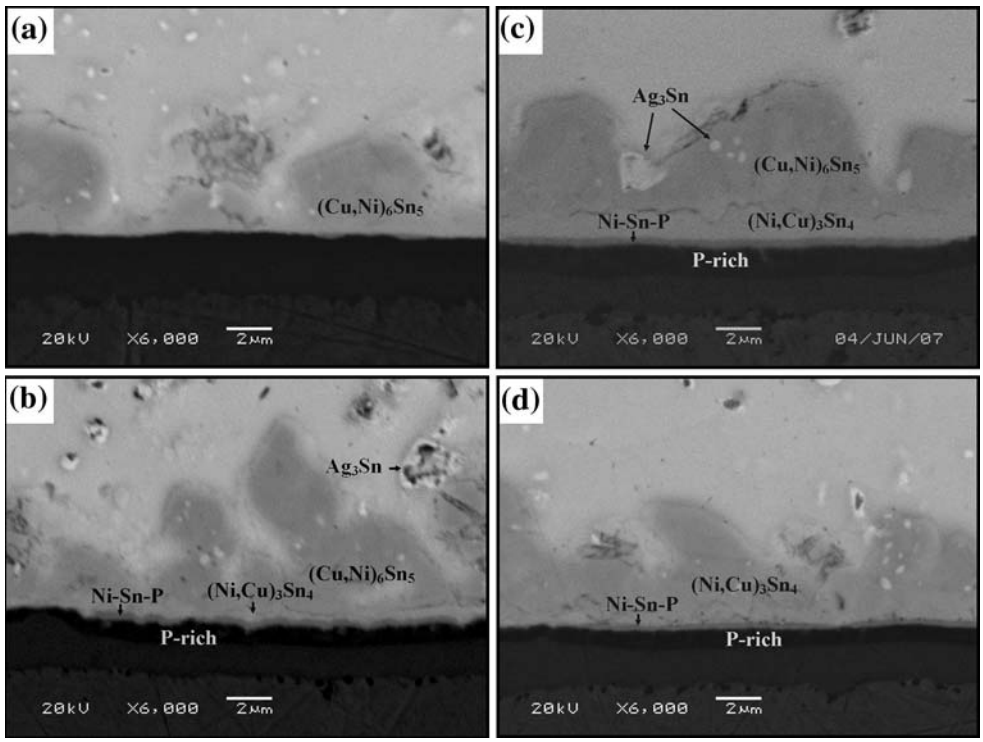

Fig. 4 Microstructure of Sn-3Ag-0.5Cu solder interface after various aging times: (a) 100 h, (b) 500 h, (c) 1000 h, and (d) 1500 h

(Liquid) + $(Cu,Ni)_6Sn_5$ + $(Ni,Cu)_3Sn_4$, and two two-phase fields, (Liquid) + $(Ni,Cu)_3Sn_4$ and (Liquid) + $(Cu,Ni)_6Sn_5$. Note that the (Liquid) single-phase field is very small in size, and this is the reason why a small change in Cu and/or Ni concentration can produce completely different results. This also indicates that with a very high Cu concentration, $(Cu,Ni)_6Sn_5$ is the first IMC to form next to the Sn phase, because Ni is dissolved into the solder where the Cu-to-Sn ratio remains unchanged. This is owing to the fact that dissolution of Ni to liquid solder is much faster than the diffusion of Cu or Sn

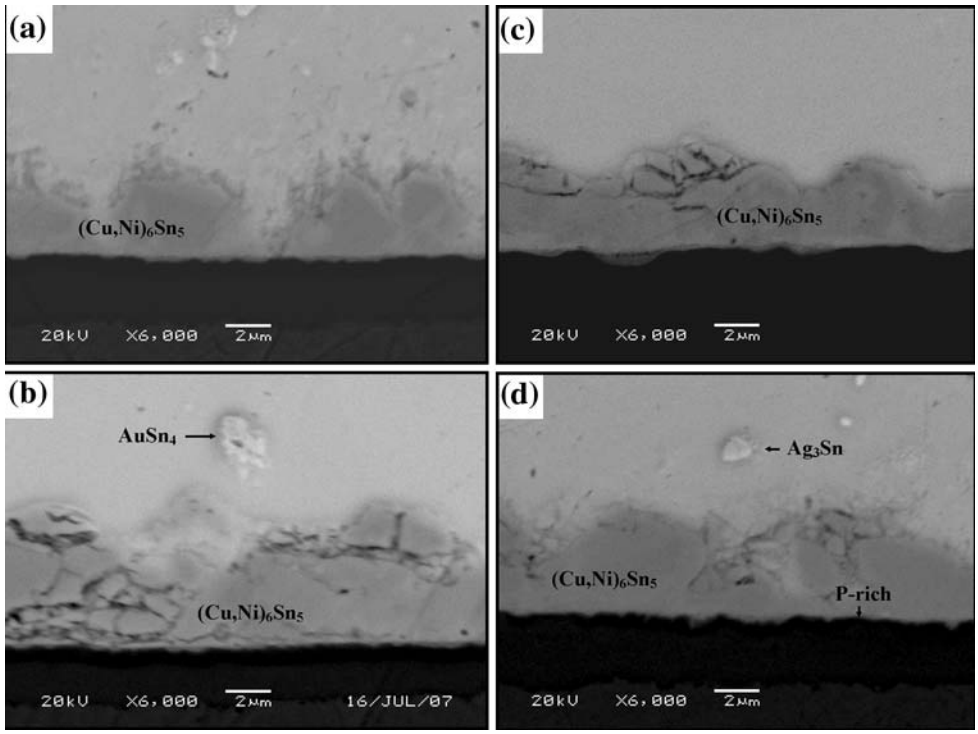

Fig. 5 Microstructure of Sn-1Ag-0.5Cu solder interface after various aging times: (a) 100 h, (b) 500 h, (c) 1000 h, and (d) 1500 h

Table 1 Compositions of IMCs formed at the interface between Ni-P layer and Sn-*x*Ag-0.5Cu solder after various aging times

Aging time at 150 °C	Sn-1Ag-0.5Cu	Sn-3Ag-0.5Cu	Sn-4Ag-0.5Cu
0 h	$(Cu,Ni)_6Sn_5$	$(Cu,Ni)_6Sn_5$	$(Cu,Ni)_6Sn_5$
100 h	$(Cu,Ni)_6Sn_5$	$(Cu,Ni)_6Sn_5$	$(Cu,Ni)_6Sn_5$/ $(Ni,Cu)_3Sn_4$
500 h	$(Cu,Ni)_6Sn_5$	$(Cu,Ni)_6Sn_5$/ $(Ni,Cu)_3Sn_4$	$(Ni,Cu)_3Sn_4$
1000 h	$(Cu,Ni)_6Sn_5$	$(Cu,Ni)_6Sn_5$/ $(Ni,Cu)_3Sn_4$	$(Ni,Cu)_3Sn_4$
1500 h	$(Cu,Ni)_6Sn_5$	$(Ni,Cu)_3Sn_4$	$(Ni,Cu)_3Sn_4$

into Ni that has to take place via solid-state mechanism (Ref 7). Additionally, for the Sn-4Ag-0.5Cu, after aging for 100 h, a thin layer of $(Ni,Cu)_3Sn_4$ was present between $(Cu,Ni)_6Sn_5$ and the Ni-P layer. After aging over 500 h, the formed interfacial IMCs changed to single $(Ni,Cu)_3Sn_4$. It is presumably related to the available Cu content in the solder matrix. The source of Cu in the bulk solder is not infinite. During IMCs growth at the interface, the concentration of Cu in the bulk solder will be gradually decreased (Ref 9). As a result, the interfacial reaction products change from $(Cu,Ni)_6Sn_5$ to $(Cu,Ni)_6Sn_5$ + $(Ni,Cu)_3Sn_4$, and then to $(Ni,Cu)_3Sn_4$, due to the restriction of supply of Cu atoms from the solder to interface. However, for the Sn-3Ag-0.5Cu and Sn-1Ag-0.5Cu, the reaction at the interface between the solder and the Ni-P layer after aging at 150 °C differs markedly from that which had been observed in the Sn-4Ag-0.5Cu specimens. The interfacial $(Ni,Cu)_3Sn_4$ IMCs in the Sn-3Ag-0.5Cu form very slowly. Moreover, no $(Ni,Cu)_3Sn_4$ IMC is

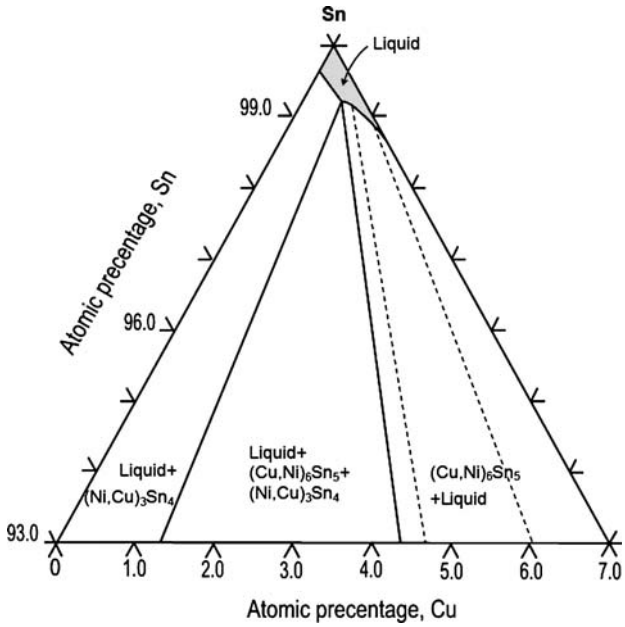

Fig. 6 The Cu-Ni-Sn ternary isotherm at 235 °C. This isotherm was adapted from Laurila et al. (Ref 7)

observed at the interfaces of the Sn-1Ag-0.5Cu specimens, although they are present in the Sn-4Ag-0.5Cu and Sn-3Ag-0.5Cu specimens. This result indicates that the formation of the interfacial $(Ni,Cu)_3Sn_4$ IMCs is clearly inhibited because the Ag content in the Sn-*x*Ag-0.5Cu alloys decreases. However, the inhibition mechanism is still unclear. In this study, the average Cu contents in the Sn-Ag-Cu solders were fixed at 0.5 wt.%.

The interfacial $(Cu,Ni)_6Sn_5$ IMC layers were formed due to the diffusion of Cu atoms from bulk solder to interface. However, the conclusion by Jeon et al. (Ref 14) indicated that diffusion of Sn or Cu atoms becomes difficult during aging because the diffusion path will be through bulky layers of IMCs or grain boundaries of IMCs. Thus, the inhibition of interfacial $(Ni,Cu)_3Sn_4$ IMC formation for Sn-1Ag-0.5Cu solder joints might be attributed to the fact that Cu atoms can easily diffuse from the bulk solder to the interface. The amount of the matrix IMCs (Ag_3Sn and Cu_6Sn_5) in the Sn-1Ag-0.5Cu specimens is much less than in the Sn-4Ag-0.5Cu and Sn-3Ag-0.5Cu. Further studies are needed to elucidate this phenomenon.

Figure 7 plots the pull force vs. the reaction time for the solder balls on the Ni-P layer. The results reveal that the as-reflowed Sn-1Ag-0.5Cu, Sn-3Ag-0.5Cu, and Sn-4Ag-0.5Cu solder balls have different pull forces of 5.3, 6.5, and 7.8 N, respectively. These results show that the Ag content dominates the bond strength of as-reflowed Sn-*x*Ag-0.5Cu samples. The pull forces of all samples decreased with aging time at 150 °C. The Sn-4Ag-0.5Cu solder joint was stronger after aging for 100-500 h than the Sn-3Ag-0.5Cu and Sn-1Ag-0.5Cu solder joints in the pull tests. However, after aging for 1000-1500 h, Sn-4Ag-0.5Cu and Sn-3Ag-0.5Cu solder joints had similar pull forces which still exceeded that of the Sn-1Ag-0.5Cu solder joint.

After ball pull testing, failure mode analysis of each test conditions was performed within a SEM system. In a previous study (Ref 10), two typical fracture modes become evident at different locations from those identified. One typical fracture mode is fracture through the solder matrix, as presented in Fig. 8(a), and the other is fracture along the interface between the solder and the Ni-P layer, as presented in Fig. 8(b). Accordingly, failure modes can be classified as solder fracture and interface fracture. For each test sample a fracture mode map was prepared and the percentage of joints showing solder and interface fracture according to the above criterion was used to evaluate the quality of the solder joints. Figure 9 presents statistical charts for the pull test fracture modes for aging treatment. Fracture surface analyses based on pull tests reveal fracture through the solder matrix of as-reflowed samples. When three Sn-*x*Ag-0.5Cu solder joints were aged at 150 °C, the fracture modes yielded different results. For Sn-4Ag-0.5Cu solder joints, fracture occurred along the interface between the solder and the Ni-P layer in specimens that were aged for more than 100 h. For Sn-3Ag-0.5Cu solder joints, fracture occurred along the interface in specimens that were aged over 500 h. However, only solder matrix fracture occurred in Sn-1Ag-0.5Cu specimens that had been aged at 100-1500 h.

Figure 10(a) presents SEM micrographs of the solder matrix fracture mode. Clear necking occurred in the solder, and the fracture surface showed dimpled morphology, indicating that the fracture behavior was ductile. Figure 10(b) presents fracture inside the interfacial IMC layer. The whole fracture surface was relatively flat, indicating macroscopically brittle behavior. The EDX analysis on the broken surfaces further verified that failure occurred along the $(Ni,Cu)_3Sn_4$ IMCs. Additionally, between the fracture modes in Fig. 9 and the interfacial IMC phases in Table 1, the interface fracture mode relates to the formation of interfacial $(Ni,Cu)_3Sn_4$ IMCs. The results reveal that the fracture mode is shifted from solder matrix failure to interface fracture with formation of the interfacial $(Ni,Cu)_3Sn_4$ IMCs layer. Other researchers have reported this brittle fracture (along the interface) (Ref 17). On the other hand, when the ductile fracture occurs in a solder matrix, the decrease in strength is caused by IMCs coarsening in the solder matrix as aging time increases. However, a comparison of pull force (Fig. 7) and fracture modes (Fig. 9) indicates that pull force decreases as the aging time increases and the gradients of the curves drop significantly when interface fracture occurs. Therefore, the much higher rate of degradation of the pull strengths of the interface fracture mode than the solder matrix fracture mode is attributable to the brittleness of the interfacial IMCs layer. The above analysis indicates that during aging, the formation of interfacial $(Ni,Cu)_3Sn_4$ IMCs layers strongly influences the bond strength and the fracture behavior of a solder joint. This fact demonstrates that interfacial layers are key to understanding the changes in bond strength.

During aging, the pull force of the Sn-1Ag-0.5Cu solder joint decreases more slowly than that of Sn-3Ag-0.5Cu and Sn-4Ag-0.5Cu solder joints, indicating that the pull force of the Sn-1Ag-0.5Cu solder joint is degraded by about 21% by aging, which is less than the degradation for Sn-3Ag-0.5Cu (28%) and Sn-4Ag-0.5Cu (40%). Therefore, unlike the pull force of the Sn-3Ag-0.5Cu and Sn-4Ag-0.5Cu solder joints, the pull force of Sn-1Ag-0.5Cu solder joints is not sensitive to extended aging time, such as 1500 h, at 150 °C.

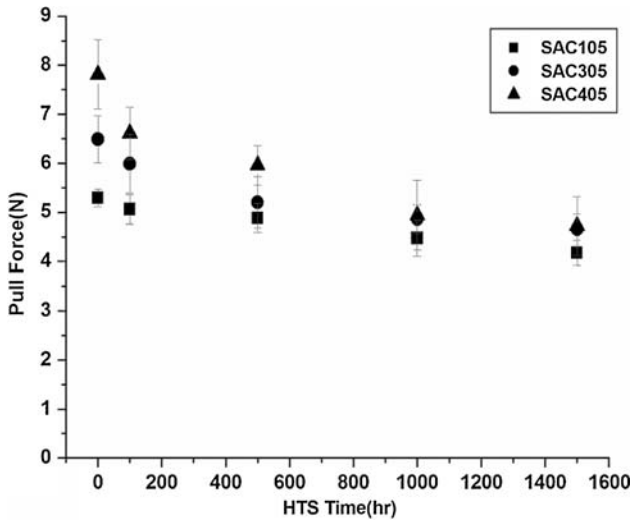

Fig. 7 Pull forces of Sn-*x*Ag-0.5Cu solder balls with Ni-P layer after aging at 150 °C for various time periods

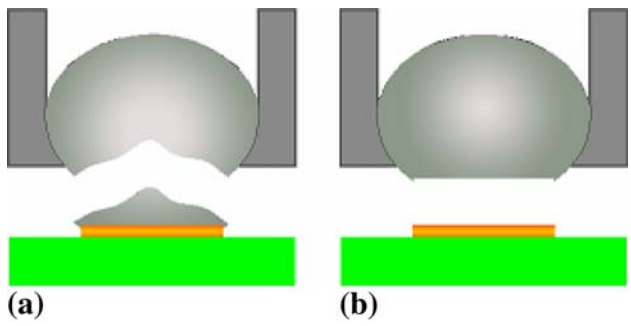

Fig. 8 Schematic drawing of fracture modes for pull strength tests: (a) solder fracture and (b) interface fracture

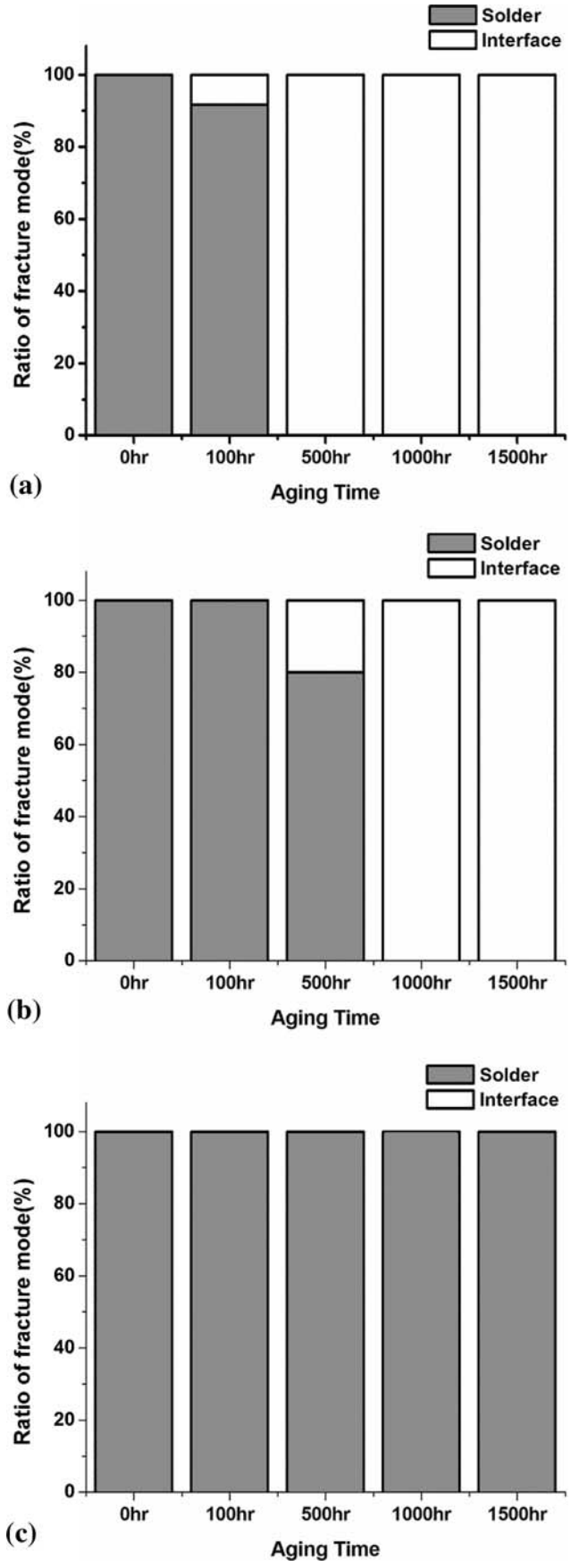

Fig. 9 Ball pull fracture modes of the Sn-*x*Ag-0.5Cu solder joints: (a) Sn-4Ag-0.5Cu, (b) Sn-3Ag-0.5Cu, and (c) Sn-1Ag-0.5Cu

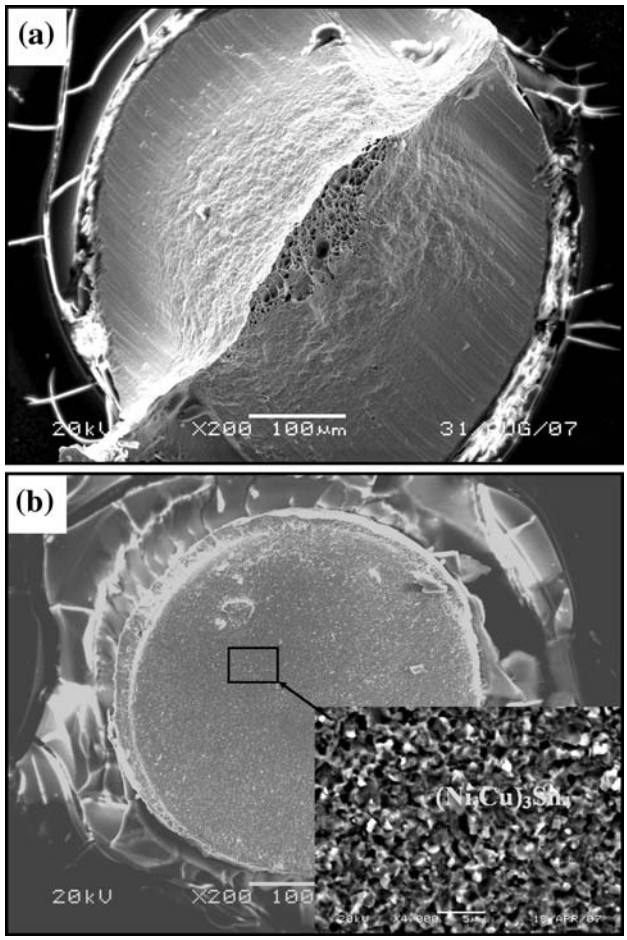

Fig. 10 Fracture surface in Sn-3Ag-0.5Cu solder joints: (a) aged for 100 h (solder fracture mode) and (b) aged for 1000 h (interface fracture mode)

4. Conclusion

The only interfacial IMC layer in the as-reflowed specimens was $(Cu,Ni)_6Sn_5$ IMCs for Sn-*x*Ag-0.5Cu solders. The morphologies of the interfacial IMCs during aging at 150 °C differed remarkably. The $(Ni,Cu)_3Sn_4$ IMCs layer formed when Sn-4Ag-0.5Cu and Sn-3Ag-0.5Cu solders were used as aging time increased over 100 and 500 h, respectively. However, only $(Cu,Ni)_6Sn_5$ IMCs formed in Sn-1Ag-0.5Cu solders, when the aging time was extended beyond 1500 h.

For as-reflowed specimens with three Ag contents, the amount of Ag_3Sn IMCs in the solder matrix influences the bond strength. Additionally, after aging at 150 °C, two factors are expected to influence pull strength and fracture modes. One factor is the formation of brittle $(Ni,Cu)_3Sn_4$ IMCs at the interface, and the fact that fracture occurs along the interface. The other factor is the coarsening of Ag_3Sn IMCs in the solder matrix, resulting in softening which led to ductile fracture of the solder balls. However, the pull force decreases as the aging time increases and the gradients of the pull force versus aging time curves drop significantly when interface fracture occurs. Therefore, the much higher degradation rate of the pull strengths of both Sn-3Ag-0.5Cu (28%) and Sn-4Ag-0.5Cu (40%) solders than that of the specimens of Sn-1Ag-0.5Cu (21%) solder should be attributed to the brittleness of the

interfacial IMC layer, indicating that the pull strength of the Sn-1Ag-0.5Cu solder joints is not sensitive to extended aging time.

References

1. C.E. Ho, R.Y. Tsai, Y.L. Lin, and C.R. Kao, Effect of Cu Concentration on the Reactions Between Sn-Ag-Cu Solders and Ni, *J. Electron. Mater.*, 2002, **31**(6), p 584–590
2. W.C. Luo, C.E. Ho, J.Y. Tsai, Y.L. Lin, and C.R. Kao, Solid-State Reactions Between Ni and Sn-Ag-Cu Solders with Different Cu Concentrations, *Mater. Sci. Eng. A*, 2005, **396**, p 385–391
3. J.W. Yoon, S.W. Kim, and S.B. Jung, IMC Morphology, Interfacial Reaction and Joint Reliability of Pb-Free Sn-Ag-Cu Solder on Electrolytic Ni BGA Substrate, *J. Alloys Compd.*, 2005, **392**, p 247–252
4. K. Zeng and K.N. Tu, Six Cases of Reliability Study of Pb-Free Solder Joints in Electronic Packaging Technology, *Mater. Sci. Eng. R*, 2002, **38**, p 55–105
5. J.H. Kim, S.W. Jeong, H.D. Kim, and H.M. Lee, Morphological Transition of Interfacial Ni_3Sn_4 Grains at the Sn-3.5Ag/Ni Joint, *J. Electron. Mater.*, 2003, **32**(11), p 1228–1234
6. D.G. Kim, J.W. Kim, and S.B. Jung, Effect of Aging Conditions on Interfacial Reaction and Mechanical Joint Strength Between Sn-3.0Ag-0.5Cu Solder and Ni-P UBM, *Mater. Sci. Eng. B*, 2005, **121**, p 204–210
7. T. Laurila, V. Vuorinen, and J.K. Kivilahti, Interfacial Reactions Between Lead-Free Solders and Common Base Materials, *Mater. Sci. Eng. R*, 2005, **49**, p 1–60
8. P. Sun, C. Andersson, X. Wei, Z. Cheng, D. Shangguan, and J. Liu, High Temperature Aging Study of Intermetallic Compound Formation of Sn-3.5Ag and Sn-4.0Ag-0.5Cu Solders on Electroless Ni(P) Metallization, *J. Alloys Compd.*, 2006, **425**, p 191–199
9. J.W. Yoon, W.C. Moon, and S.B. Jung, Interfacial Reaction of ENIG/Sn-Ag-Cu/ENIG Sandwich Solder Joint During Isothermal Aging, *Microelectron. Eng.*, 2006, **83**, p 2329–2334
10. C.N. Hwang, K. Suganuma, M. Kiso, and S. Hashimoto, Influence of Cu Addition to Interface Microstructure Between Sn-Ag Solder and Au/Ni-6P Plating, *J. Electron. Mater.*, 2004, **33**(10), p 1200–1209
11. M. He, Z. Chen, and G. Qi, Solid State Interfacial Reaction of Sn-37Pb and Sn-3.5Ag Solders with Ni-P Under Bump Metallization, *Acta Mater.*, 2004, **52**, p 2047–2056
12. M. He, W.H. Lau, G. Qi, and Z. Chen, Intermetallic Compound Formation Between Sn-3.5Ag Solder and Ni-Based Metallization During Liquid State Reaction, *Thin Solid Films*, 2004, **462**, p 376–383
13. M.O. Alam, Y.C. Chan, and K.C. Hung, Reliability Study of the Electroless Ni-P Layer Against Solder Alloy, *Microelectron. Reliab.*, 2002, **42**, p 1065–1073
14. Y.D. Jeon, S. Nieland, A. Ostmann, H. Reichl, and K.W. Paik, A Study on Interfacial Reactions Between Electroless Ni-P Under Bump Metallization and 95.5Sn-4.0Ag-0.5Cu Alloy, *J. Electron. Mater.*, 2003, **32**(6), p 548–557
15. M.L. Huang, T. Loeher, D. Manessis, L. Boettcher, A. Ostmann, and H. Reichl, Morphology and Growth Kinetics of Intermetallic Compounds in Solid-State Interfacial Reaction of Electroless Ni-P with Sn-Based Lead-Free Solders, *J. Electron. Mater.*, 2006, **35**(1), p 181–188
16. J.W. Yoon, S.W. Kim, J.M. Koo, D.G. Kim, and S.B. Jung, Reliability Investigation and Interfacial Reaction of Ball-Grid-Array Packages Using the Lead-Free Sn-Cu Solder, *J. Electron. Mater.*, 2004, **33**(10), p 1190–1199
17. Z. Chen, M. He, A. Kumar, and G.J. Qi, Effect of Interfacial Reaction on the Tensile Strength of Sn-3.5Ag/Ni-P and Sn-37Pb/Ni-P Solder Joints, *J. Electron. Mater.*, 2007, **36**(1), p 17–25